

# Formation of Nickel Based Ohmic Contact to High Energy Vanadium Implanted n-Type 4H-SiC\*

Wang Chao<sup>†</sup>, Zhang Yimen, Zhang Yuming, Guo Hui, Xu Daqing, and Wang Yuehu

(Key Laboratory of the Ministry of Education for Wide Band-Gap Semiconductor Materials and Devices, Microelectronics Institute, Xidian University, Xi'an 710071, China)

**Abstract:** The diffusion behavior of vanadium (V) implanted in SiC is investigated by secondary ion mass spectrometry. Significant redistribution, especially out-diffusion of vanadium towards the sample surface, is not observed after 1650°C annealing. Higher carrier concentration is obtained due to a lack of compensation of vanadium in the surface region. The electrical characteristics of Ni contacts to V-implanted n-type 4H-SiC are investigated using a linear transmission line method. A specific contact resistance as low as  $4.4 \times 10^{-3} \Omega \cdot \text{cm}^2$  is achieved after annealing at 1050°C for 10min in gas ambient consisting of 90% N<sub>2</sub> and 10% H<sub>2</sub>. X-ray diffraction analysis shows the formation of Ni<sub>2</sub>Si and graphite phase at the interface after annealing. This provides the evidence that the carbon vacancies, resulting from the out-diffusion of carbon atoms from SiC, contribute to the formation of ohmic contact through the reduction of effective Schottky barrier height for the transport of electrons.

**Key words:** ohmic contact; semi-insulating SiC; V ion implantation; diffusion; carbon vacancies

**PACC:** 7340C; 6170T; 6170W

**CLC number:** TN304

**Document code:** A

**Article ID:** 0253-4177(2007)11-1701-05

## 1 Introduction

Silicon carbide (SiC) is an excellent material for high-temperature, high-frequency, and high-power semiconductor devices and has demonstrated its great potential over the past decade. Semi-insulating regions can be applied to device isolation, a key technology for integrated electronic devices in SiC ICs<sup>[1]</sup>, similar to the silicon-on-insulator (SOI) structures in Si ultra large scale ICs. Since selective doping can be made only by ion implantation due to the low diffusion coefficients of impurities in SiC, compensation implantation can be used to obtain high resistive regions for electrical isolation. Semi-insulating properties in SiC can be achieved by deep level compensating all shallow donors or acceptors, with the doping of V<sup>[2~4]</sup>. Studies show that the resistivities at room temperature exceed  $10^{12}$  and  $10^6 \Omega \cdot \text{cm}$  for V-doped in p- and n-type SiC, respectively<sup>[5~8]</sup>.

It is very difficult to fabricate ohmic contacts on high resistive SiC material. To reduce the con-

tact resistance of ohmic contacts, a heavily doped layer was grown at the top of a V-implanted SiC sample by Kimoto *et al.*<sup>[5]</sup>. This technology can be simplified by using high energy implantation, which makes most vanadium ions locate in deeper regions. As a result, a higher free-carrier concentration is attained in the surface region due to the lack of compensation. However, the diffusion behavior of vanadium in SiC after high-temperature annealing remains unclear. In our previous works, a resistivity as high as  $7.6 \times 10^6 \Omega \cdot \text{cm}$  was obtained for high energy (2.1MeV) vanadium implanted n-type 4H-SiC<sup>[7,8]</sup>. Nickel based metals have been demonstrated to be a superior ohmic contact to n-type SiC<sup>[9,10]</sup>. However, the actual formation mechanism is not clear yet.

In this paper, the processes and measurements of contact resistance on V-implanted n-type 4H-SiC layers are presented in detail. Secondary ion mass spectrometry (SIMS) is used to study the redistribution of vanadium in n-type 4H-SiC after high-temperature annealing. The electrical characteristics of Ni based ohmic contacts to n-type

\* Project supported by the National Natural Science Foundation of China (No.60376001), the State Key Development Program for Basic Research of China (No.2002CB311904), and the National Defense Basic Research Program of China (No.51327020202)

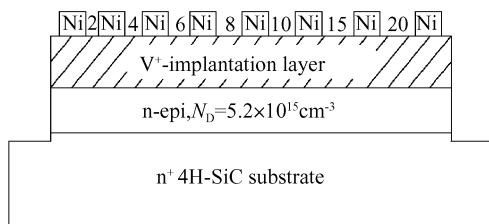
<sup>†</sup> Corresponding author. Email:chwang@mail.xidian.edu.cn

Received 26 May 2007, revised manuscript received 4 July 2007

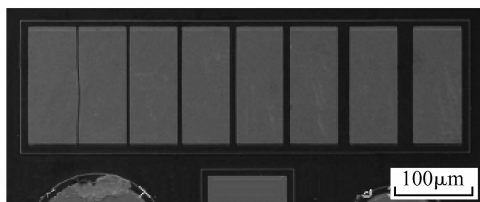
SiC are investigated by the linear transmission line method (TLM). X-ray diffraction (XRD) is used to identify the phase formation in the annealed contacts.

## 2 Experiment

The wafers used in this work were  $4.9\mu\text{m}$ -thick n-type ( $5.2 \times 10^{15} \text{cm}^{-3}$ ) 4H-SiC epitaxial layers grown on Si face,  $8^\circ$  off-axis, (0001)-oriented n-type 4H-SiC substrates, purchased from Cree, Inc. V ions were implanted with a  $1.4 \times 10^{13} \text{cm}^{-2}$  dose at 2100keV. An activation annealing was carried out in Ar ambient at  $1650^\circ\text{C}$  for 30min. To minimize Si evaporation from the sample surface, the samples were encased in a SiC-coated graphite crucible during annealing. Then, the samples were processed into a rectangular mesa structure by reactive ion etching with  $\text{CF}_4$  and  $\text{O}_2$  gases. The size of the rectangular mesa was  $565\mu\text{m} \times 170\mu\text{m}$ . Prior to metal deposition, the samples were cleaned in acetone and deionized water followed by a standard RCA procedure, and then patterned with photoresist. The TLM structures were photolithographically prepared on the rectangular mesa. Ni was deposited and patterned by lift-off on the samples. The size of the rectangular Ni pads was  $60\mu\text{m} \times 150\mu\text{m}$ , and the spaces between pads were 2, 4, 6, 8, 10, 15, and  $20\mu\text{m}$ , respectively. Figure 1 (a) shows a cross section of a linear TLM structure with seven unequal spaces



(a)



(b)

Fig.1 (a) A linear TLM structure with seven unequal spaces between the contact pads. All distances are given in  $\mu\text{m}$ ; (b) SEM image of this structure

between the contacts. Finally, the contacts were annealed at  $1050^\circ\text{C}$  for 10min in a gas ambient consisting of 90%  $\text{N}_2$  and 10%  $\text{H}_2$ . The TLM pattern image of the scanning electron microscope (SEM) is shown in Fig.1 (b).

Depth profiles of the V-implanted SiC samples were obtained by SIMS using a CAMECA-ims-4f instrument with a  $10.5\text{keV O}_2^+$  primary ion beam. The primary beam current of  $1\mu\text{A}$  was focused and rastered over an area of  $250\mu\text{m} \times 250\mu\text{m}$ . The secondary ion signal was extracted from a circular area of  $60\mu\text{m}$  in diameter centered on the rastered region. The depth scales were determined by measuring the total crater depth with a surface profiler and we assumed a constant sputtering rate during depth profiling. The concentration scales were determined by assuming that the stated nominal implantation fluence is correct.

The specific contact resistance and sheet resistance measurements were performed on the TLM structures at room temperature by an HP4156B semiconductor parameter analyzer. To better study the phase formation at the interface during annealing, XRD analysis was performed using a SHIMADZU XRD-7000 instrument with  $\text{CuK}\alpha$  radiation at 40kV and 40mA. The resulting data were analyzed with graphical-overlay software.

## 3 Results and discussion

### 3.1 SIMS results

The SIMS depth profiles of vanadium implanted in SiC before and after annealing are shown in Fig. 2. As implanted profiles in SiC samples, the near surface tail and the mean concentration are well reproduced by the Monte Carlo TRIM simulation. However, the tail in the bulk of the epilayer extends to deeper regions than that of the simulated profile. Channeling effects, which are not considered in TRIM, are assumed to be responsible for the observed discrepancy<sup>[11]</sup>.

A little in-diffusion tail extending to the deeper region is observed after  $1650^\circ\text{C}$  annealing. In addition, a slight movement of the peak of implanted V concentration towards the surface can be seen. Out-diffusion of vanadium towards the sample surface can be better visualized in the in-

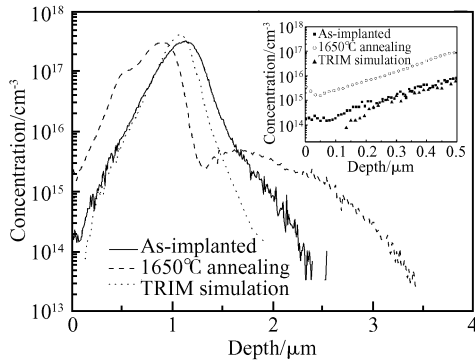


Fig.2 SIMS depth profiles for V-implanted 4H-SiC. The inset shows the distribution of vanadium ions in the surface region.

set. Out-diffusion results in a slight pile up of vanadium in the surface region, but it is not pronounced. Considering the incomplete ionization effect, the activated vanadium ions concentration is below  $10^{15} \text{ cm}^{-3}$ . As a result, the free-carrier concentration remains unchanged ( $\sim 5.2 \times 10^{15} \text{ cm}^{-3}$ ) due to the lack of vanadium ions compensation in the surface region of SiC.

### 3.2 TLM measurements

The specific contact resistance  $\rho_c$  is defined by the local current density  $j$  and the local voltage drop  $V$  as

$$\rho_c = \left[ \left( \frac{\partial j}{\partial V} \right)_{V=0} \right]^{-1} \quad (1)$$

Since the current distribution across a contact area is usually not homogeneous,  $\rho_c$  cannot be directly measured, but must be extracted with special test structures<sup>[12]</sup>. By employing the commonly used TLM originally proposed by Shockley, one determines the resistance between two rectangular contact pads of length  $d$  and width  $W$  on an insulation mesa of width  $W + 2\delta$  with respect to the spacing  $L$  between the contacts (see Fig. 3).

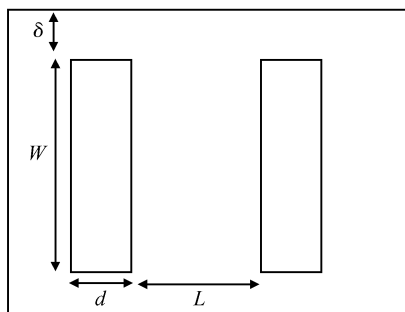


Fig. 3 Geometry of a linear TLM structure

The total resistance  $R_T$  as a function of  $L$  is shown in Fig. 4. In order to reduce the errors, the data shown in Fig. 4 are the median values from multiple measurements. By assuming that the length of each contact is long enough ( $W \gg \delta$ ), the total resistances  $R_T$  can be described by

$$R_T = 2R_c + \frac{R_{sh}L}{W} \quad (2)$$

where  $2R_c$  is obtained from the intercept on the  $y$  axis. The specific contact resistance  $\rho_c$  can be calculated as

$$\rho_c = \frac{(R_c W)^2}{R_{sh}} \quad (3)$$

Therefore, sheet resistance  $R_{sh}$  is  $W$  multiplied by the slope  $dR_T/dL$  of the linear curve shown in Fig. 4. The value for sheet resistance  $R_{sh}$  of the implanted layer is about  $68.8 \text{ k}\Omega/\square$ . The lowest value of the specific contact resistance is  $4.4 \times 10^{-3} \Omega \cdot \text{cm}^2$ . Lower contact resistance can be obtained for SiC samples with higher initial carrier concentration. Semi-insulating SiC layers formed by this technique can be effectively used for device isolation, reduction of parasitic impedance in high-frequency devices, and the realization of SiC ICs on insulators.

The transport of electrons from metal to SiC can be described through the thermionic emission model because of the low doping concentration ( $n = 5.2 \times 10^{15} \text{ cm}^{-3}$ ). The Schottky barrier height,  $\phi_{Bn}$ , was previously calculated to be  $0.35 \text{ eV}$  for Ni contact on n-type 4H-SiC after high-temperature annealing<sup>[13]</sup>. When the  $\phi_{Bn} = 0.35 \text{ eV}$  and the Richardson contact<sup>[14]</sup>,  $A^* = 146 \text{ A}/(\text{cm}^2 \cdot \text{K}^2)$ , are substituted into  $\rho_c = (k/qA^*T) \times \exp(q\phi_{Bn}/kT)$ , the specific contact resistance  $\rho_c$  is calculated to be  $1.5 \times 10^{-3} \Omega \cdot \text{cm}^2$ , which agrees well with the experimental value.

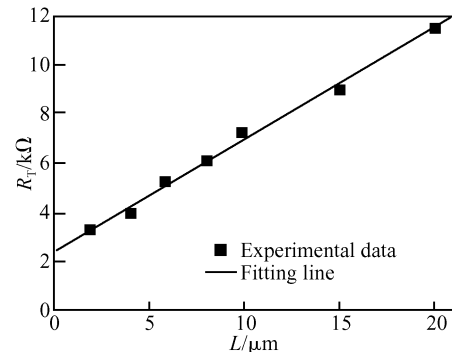


Fig. 4 TLM total resistance versus gap spacing

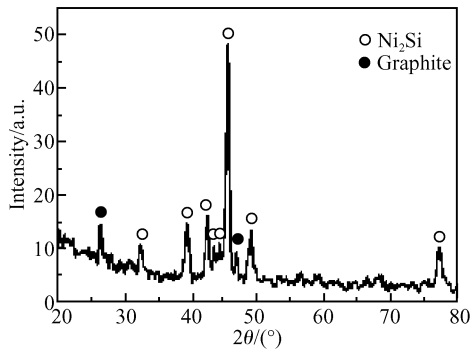


Fig.5 X-ray diffraction pattern of Ni contact to n-type 4H-SiC after annealing at 1050°C for 30min

### 3.3 XRD analysis

Figure 5 shows the results of XRD analysis after 1050°C annealing. A dominant peak with many small peaks at positions corresponding to  $\text{Ni}_2\text{Si}$  appears in the data range. In addition, two peaks corresponding to graphite are also detected.

It is well established that nickel silicides are formed during high-temperature annealing as a result of SiC dissociation and the chemical reaction between Ni and Si<sup>[15,16]</sup>. The depth profiles of Ni, Si, and C atoms support that the silicidation occurred at the interface of Ni with SiC and proceeded by means of the out-diffusion of Si rather than the in-diffusion of Ni<sup>[17]</sup>. In addition, the silicidation through out-diffusion of Si is faster than out-diffusion of C, leaving elemental C atoms at the interface in the form of a nanocrystalline graphite film<sup>[15,18]</sup>. The XRD results agree well with the results obtained by Han *et al.*<sup>[17]</sup>.

Studies including XRD<sup>[19]</sup>, Raman<sup>[16]</sup>, X-ray energy-dispersive spectrometer (XDES)<sup>[18]</sup>, synchrotron radiation photoemission spectroscopy (SRPES)<sup>[17]</sup>, and morphological characterization<sup>[20]</sup> show that the ohmic behavior of Ni based contact to n-type 4H-SiC is strongly related to the out-diffusion of carbon atoms rather than  $\text{Ni}_2\text{Si}$ . The  $\text{Ni}_2\text{Si}$  contact produced at 600°C annealing shows a rectifying behavior<sup>[10]</sup>, as shown in Fig. 6 (a). However, a number of  $V_C$  are formed due to the out-diffusion of carbon atoms when the Ni contact is annealed at 950°C or above. This causes the net concentration of electrons to increase under the contact because of the role of  $V_C$  acting as donors for electrons<sup>[21]</sup>. Therefore, the depletion layer width and effective tunneling barrier height for the transport of electrons are simultaneously

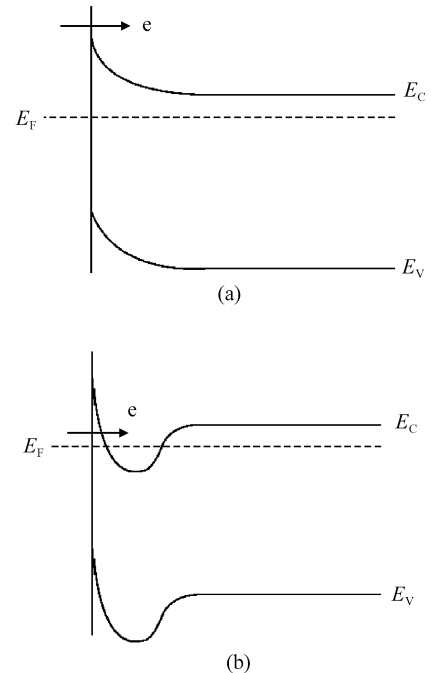


Fig.6 Energy band diagrams under Ni contact (a) After annealed at 600°C ;(b) After annealed at 1050°C

decreased<sup>[19]</sup>, leading to the reduction of contact resistivity, as shown in Fig. 6 (b).

## 4 Conclusions

The V atom profiles measured by SIMS show a slight redistribution after high-temperature annealing at 1650°C. However, a strong pile up of vanadium in the surface region of SiC is not observed, indicating that the carrier concentration remains unchanged in the surface region due to the lack of compensation. Semi-insulating SiC layers formed by this technique can be effectively used for device isolation and the realization of SiC ICs on insulators. Ni based n-type 4H-SiC ohmic contact with the specific contact resistance  $\rho_c$  as low as  $4.4 \times 10^{-3} \Omega \cdot \text{cm}^2$  is achieved on the high energy V-implanted SiC surface. XRD analysis shows the formation of  $\text{Ni}_2\text{Si}$  and graphite at the Ni/SiC interface after 1050°C annealing, which supports the fact that the formation of C vacancies is responsible for the low resistance contact.

## References

- [1] Arai M, Ono S, Kimura C. IMPATT oscillation in SiC p<sup>+</sup>-n-n<sup>+</sup> diodes with a guard ring formed by vanadium ion implantation. Electron Lett, 2004, 40(16):1026

- [2] Bickermann M, Weingartner R, Winnacker A. On the preparation of vanadium doped PVT grown SiC boules with high semi-insulating yield. *J Cryst Growth*, 2003, 254: 390
- [3] Zvanut M E, Lee W, Mitchel W C, et al. The acceptor level for vanadium in 4H and 6H SiC. *Physica B*, 2006, 376/377: 346
- [4] Tamulaitis G, Yilmaz I, Shur M S, et al. Carrier lifetime in conductive and vanadium-doped 6H-SiC substrates. *Appl Phys Lett*, 2004, 84(3): 335
- [5] Kimoto T, Nakajima T, Matsunami H, et al. Formation of semi-insulating 6H-SiC layers by vanadium ion implantations. *Appl Phys Lett*, 1996, 69(8): 1113
- [6] bickermann M, Hofmann D, Straubinger T L, et al. On the preparation of semi-insulating SiC bulk crystals by the PVT technique. *Appl Sur Sci*, 2001, 184: 84
- [7] Wang Chao, Zhang Yuming, Zhang Yimen. Characteristics of semi-insulating 4H-SiC layers by vanadium ion implantation. *Chinese Journal of Semiconductors*, 2006, 27(8): 1396
- [8] Wang Chao, Zhang Yimen, Zhang Yuming. Electrical and optical characteristics of vanadium in 4H-SiC. *Chin Phys*, 2007, 16(5): 1417
- [9] Crofton J, Porter L M, Williams J R. The physics of ohmic contacts to SiC. *Phys Status Solidi B*, 1997, 202: 581
- [10] Lu Weijie, Mitchel W C, Landis G R, et al. Ohmic contact properties of Ni/C film on 4H-SiC. *Solid-State Electron*, 2003, 47: 2001
- [11] Henkel T, Tanaka Y, Kobayashi N, et al. Diffusion of implanted beryllium in silicon carbide studied by secondary ion mass spectrometry. *Appl Phys Lett*, 2001, 78(2): 231
- [12] Einspruch N G, Cohen S S, Gildenblat G S. VLSI electronics microstructure science. Orlando: Academic Press, 1986
- [13] Luckowski E D, Williams J R, Bozack M J, et al. Improved nickel silicide ohmic contacts to n-type 4H and 6H-SiC using nichrome. *Mater Res Soc Symp Proc*, 1996, 423: 119
- [14] Itoh A, Kimoto T, Matsunami H. High performance of high-voltage 4H-SiC Schottky barrier diodes. *IEEE Electron Device Lett*, 1995, 16(6): 280
- [15] Nikitina I P, Vassilevski K V, Wright N G, et al. Formation and role of graphite and nickel silicide in nickel based ohmic contacts to n-type silicon carbide. *J Appl Phys*, 2005, 97(8): 083709
- [16] Kurimoto E, Harima H, Toda T, et al. Raman study on the Ni/SiC interface reaction. *J Appl Phys*, 2002, 91(12): 10215
- [17] Han S Y, Kim K H, Kim J K, et al. Ohmic contact formation mechanism of Ni on n-type 4H-SiC. *Appl Phys Lett*, 2001, 79(12): 1816
- [18] Guo Hui, Zhang Yimen, Zhang Yuming. Evidence of the role of carbon vacancies in nickel-based ohmic contacts to n-type silicon carbide. *Chinese Journal of Semiconductors*, 2007, 28(1): 5
- [19] Perez R, Mestres N, Tournier D, et al. Ni/Ti ohmic and Schottky contacts on 4H-SiC formed with a single thermal treatment. *Diamond Relat Mater*, 2005, 14: 1146
- [20] Cole M W, Joshi P C, Hubbard C W, et al. Improved Ni based composite ohmic contact to n-SiC for high temperature and high power device applications. *J Appl Phys*, 2000, 88(5): 2652
- [21] Bratus V Y, Makeeva I N, Okulov S M, et al. Positively charged carbon vacancy in 6H-SiC: EPR study. *Physica B*, 2001, 308~310: 621

## 高能量钒注入 n 型 4H-SiC 的欧姆接触形成\*

王超<sup>†</sup> 张义门 张玉明 郭辉 徐大庆 王悦湖

(西安电子科技大学微电子学院 宽禁带半导体材料与器件教育部重点实验室, 西安 710071)

**摘要:** 借助二次离子质谱法分析了注入的钒离子在碳化硅中的分布. 即使经过 1650°C 的高温退火, 钒在碳化硅中的再扩散也不显著. 退火并没有导致明显的钒向碳化硅表面扩散形成堆积的现象, 由于缺少钒的补偿作用, 表面薄层的自由载流子浓度保持不变. 采用线性传输线模型测量了钒注入 n 型 4H-SiC 上的 Ni 基接触电阻, 在 1050°C 下, 在氮、氢混合气体中退火 10min, 形成的最低比接触电阻为  $4.4 \times 10^{-3} \Omega \cdot \text{cm}^2$ . 金属化退火后的 XRD 分析结果表明, 镍、碳化硅界面处形成了  $\text{Ni}_2\text{Si}$  和石墨相. 观测到的石墨相是由于退火导致 C 原子外扩散并堆积形成, 同时在碳化硅表面形成 C 空位. C 空位可以提高有效载流子浓度, 降低势垒高度并减小耗尽层宽度, 对最终形成欧姆接触起到了关键作用.

**关键词:** 欧姆接触; 半绝缘碳化硅; 钒离子注入; 扩散; 碳空位

**PACC:** 7340C; 6170T; 6170W

**中图分类号:** TN304

**文献标识码:** A

**文章编号:** 0253-4177(2007)11-1701-05

\* 国家自然科学基金(批准号:60376001), 国家重点基础研究发展规划(批准号:2002CB311904)及国防基础研究规划(批准号:51327020202)资助项目

<sup>†</sup> 通信作者. Email: chwang@mail.xidian.edu.cn  
2007-05-26 收到, 2007-07-04 定稿